

Transient Ablation of Teflon in Intense Radiative and Convective Environments

Norio Arai*

NASA Ames Research Center, Moffett Field, Calif.

On the basis of this investigation of the high-temperature behavior of polytetrafluoroethylene (PTFE), the transient one-dimensional ablation of PTFE has been developed by taking into account the optical transmittance of both the amorphous zone and the crystalline zone of PTFE layer. Results show that although the exposed surface receded at an apparently steady state, both the internal temperature and the thickness of the gel layer increase continuously due to the internal absorption of radiation.

Nomenclature

A_p	= effective collision frequency
C_p	= fraction of mass of oxygen in a boundary layer
C_p	= specific heat
E	= activation energy
h_m	= heat of transition
h_v	= reaction heat per unit mass of oxygen
H_0	= stagnation enthalpy of the gas
H_p	= local depolymerization energy
ΔH_w	= enthalpy difference over the boundary layer
I	= radiation intensity
I_e	= external incident radiation intensity
k	= thermal conductivity
K	= absorption coefficient
L_0	= initial thickness of the ablating body
m	= index on radiation bands that penetrate the body
\dot{m}	= ablation rate
n	= index on radiation bands absorbed at the exposed surface and index of refraction
q_0	= convective heating rate without mass injection
q_r	= incident radiative heating rate at the exposed surface
q_{rad}	= total incident radiative flux absorbed at the exposed surface
Q_p	= depolymerization energy per unit volume
Q_R	= total radiation flow in the ablating body
r	= reflectivity
R	= universal gas constant
s	= position of the surface
\dot{s}	= ablation velocity, ds/dt
S	= scattering coefficient
t	= time
T	= temperature
x	= spatial coordinate
δ_{hs}	= thickness of the heat sink
ϵ	= surface emissivity
θ	= thickness of the gel layer
$\dot{\theta}$	= growing rate of the gel layer, $d\theta/dt$
ρ	= density
Ψ	= correction factor by mass injection
ξ	= transformed coordinate

Subscripts

b	= conditions at the backface
B	= blackbody
e	= external incident radiative intensity
hs	= heat sink
i	= internal reflection coefficient and interface
m	= conditions at the phase change
R	= outward direction in the ablating body
s	= surface
T	= inward direction in the ablating body
ν	= the ν th spectral band of radiation being absorbed and/or reflected at the exposed surface
1	= conditions in the gel layer
2	= conditions in the solid layer

Introduction

FOR high-speed entry of space vehicles into atmospheric environments, especially, into the large planets (e.g., Jupiter and Saturn), the aerodynamic heating is a severe one in which the radiative heating is associated with the convective heating. Ablation is a practical method for alleviating it. The ablation materials developed in the past, however, may not be adequate for alleviating the radiative heating. For such entries, ablators should be chosen to alleviate both the radiative and the convective heating.

One method uses reflecting ablation heat shields.¹⁻³ A dielectric material is used to reflect the radiative heating diffusely rather than a metallic material to reflect it specularly. The reflection by a dielectric material must be accomplished by backscattering in depth, because the surface of the probe is eroding rapidly during entry as the result of thermochemical ablation. A heat shield using a dielectric material to reflect the incident radiation avoids one of the essential inconveniences on the design that uses a metallic material; even though each metallic surface may be highly reflective, absorption always accompanies each reflection by a metallic surface. And for the absorbed radiation at the surface, the heat shield may actually behave like a blackbody in that it absorbs practically all of the incident radiation. However, a dielectric, depending on the spectral range, can be selected that absorbs essentially none of the incident radiation energy.¹

As a reflecting ablation heat shield, we may consider a few candidates, such as polytetrafluoroethylene (PTFE) and silica (SiO_2). These physical properties change abruptly at the melting point. The effects of these changes on the temperature distribution and the ablation rate, etc., are the most interesting problems. We may not know clearly the physical properties of these heat-shield materials at high temperature; however, we may know those of PTFE compared with other heat-shield materials. Experiments (at a flux level of about 1

Received Jan. 30, 1978; revision received Jan. 25, 1979. Copyright © American Institute of Aeronautics and Astronautics, Inc., 1979. All rights reserved.

Index categories: Ablation, Pyrolysis, Thermal Decomposition and Degradation (including Refractories); Radiation and Radiative Heat Transfer; Heat Conduction.

*NRC Research Associate. Present address: Institute of Space and Aeronautical Science, University of Tokyo, Tokyo, Japan. Member AIAA.

kw/cm²) have shown¹ that PTFE backscatters radiation volumetrically even when the surface is ablating. The ablation of PTFE over the melting point is not clear in the intense radiative and convective environments.

Clark⁴ first proposed the two-layer model with emphasis on the phase change of Teflon, especially on the development of the gel layer. In his investigation, the transient one-dimensional ablation was considered.

Arai applied the two-layer model to the axisymmetric model of Teflon with particular emphasis on the change in body shape and the instantaneous internal temperature distribution.⁵ He got results that are in good agreement with his experimental data.

Holzknacht took account of the influence of the order of decomposition reaction and of the thermal expansion of PTFE.⁶ Computed temperature profiles showed good agreement with measured distributions.

To the best of the author's knowledge, however, there is no paper except Kindler's,⁷ in which the effect of optical transmittance of PTFE on the temperature field and the mass loss rate are taken into account. However, it does not sufficiently explain the effect of the incident radiation.

It is the purpose of this investigation to propose numerical results of the transient thermal response of PTFE. With particular emphasis on the effect of the second-order transition of PTFE and the incident radiation on the overall behavior of the transient temperature distribution inside the heat-shield material, the formulation is made by use of the two-layer thermal model. The heat conduction equation with temperature dependent properties is coupled with the radiation transfer equation and is solved by use of the shooting method.

Analysis

Governing Equations

The one-dimensional model considered in this analysis is sketched in Fig. 1. PTFE undergoes a sharp, reversible transition at $T_m = 327^\circ\text{C}$; the transition is accompanied by a

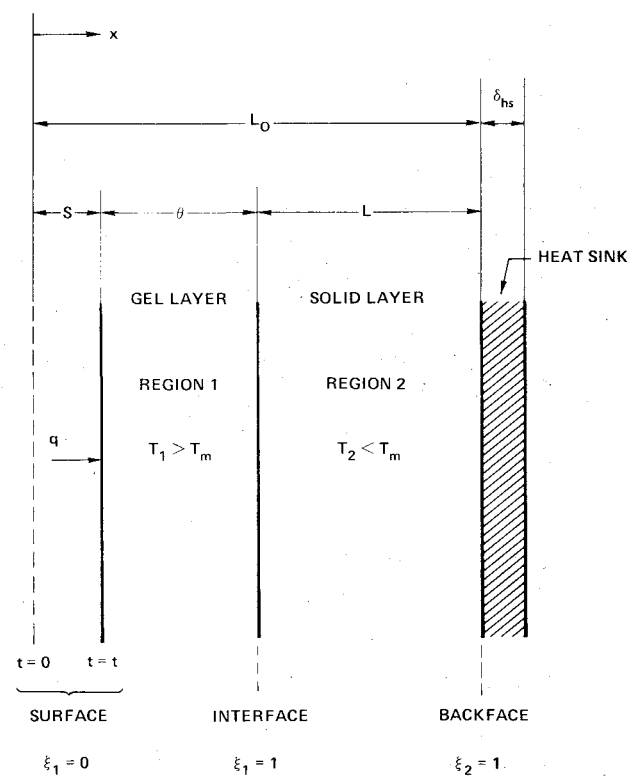


Fig. 1 Physical model.

heat of $h_m = 14$ cal/g. The phase transition plane divides the slab into two regions as shown: the gel layer (subscript 1) and the solid layer (subscript 2). As the temperature of PTFE is raised above $350\text{-}400^\circ\text{C}$, pyrolysis occurs. The polymer decomposes into gaseous products without either charring or liquid layer formation. This decomposition is not a phase transition at a constant temperature, but the depolymerization of the polymer chains. Thermal expansion is neglected in this analysis.

Conservation of energy may be expressed as

$$\rho_1 C_{p,1} \frac{\partial T_1}{\partial t} = \frac{\partial}{\partial x} \left(k_1 \frac{\partial T_1}{\partial x} \right) + Q_R + Q_P \tag{1}$$

$$\rho_2 C_{p,2} \frac{\partial T_2}{\partial t} = \frac{\partial}{\partial x} \left(k_2 \frac{\partial T_2}{\partial x} \right) + Q_R \tag{2}$$

where

$$Q_P = -A_p \rho_1 H_p(T) \exp\left(-\frac{E}{RT_1}\right)$$

$$Q_R = \pi \sum_{\nu=m}^{m'} K_{\nu} (I_{R,\nu} + I_{T,\nu} - 2n^2 I_{B,\nu})$$

Q_P is the energy per unit volume bound by the depolymerization process not only at the surface but inside the body. Q_R means the radiative term which is being absorbed and emitted in depth.

The inward and outward radiative fluxes are described by the Kubelka-Munk "two-flux" equations² as

$$\frac{dI_{T,i,\nu}}{dx} = -(S_{i,\nu} + K_{i,\nu}) I_{T,i,\nu} + S_{i,\nu} I_{R,i,\nu} + n_i^2 K_{i,\nu} I_{B,i,\nu} \tag{3}$$

$$\frac{dI_{R,i,\nu}}{dx} = (S_{i,\nu} + K_{i,\nu}) I_{R,i,\nu} - S_{i,\nu} I_{T,i,\nu} - n_i^2 K_{i,\nu} I_{B,i,\nu} \tag{4}$$

where $i=1$ for the gel layer and 2 for the solid layer. K and S are the absorption coefficient and scattering coefficient, respectively.

Boundary Conditions

We consider that the incident flux is composed of radiation bands that either penetrate the material to be backscattered in depth or are absorbed at the surface.² That is, we define the incident flux

$$q_r = \sum_{\nu=m}^{m'} q_{r,\nu} + \sum_{\nu=n}^{n'} q_{r,\nu} \tag{5}$$

where the first sum is radiation that penetrates to be scattered and the last is radiation that is absorbed at the surface. The heat transfer to the surface is reduced because of the mass transport into the boundary layer and is increased due to the exothermic reaction with the oxygen in it. Therefore, at the exposed surface, the flux conducted into the material is expressed as

$$-\left(k_1 \frac{\partial T_1}{\partial x}\right)_s = \Psi q_0 \left(1 + \frac{Ch_v}{\Delta H_w}\right) + q_{rad} \tag{6}$$

where q_0 is the convective heating rate without mass injection, Ψ is correction factor⁸ by mass injection, and q_{rad} represents the total incident radiative flux expressed as

$$q_{rad} = \pi \sum_{\nu=n}^{n'} [(1-r_{s,\nu}) I_{e,\nu} - \epsilon I_B(T_w)] \tag{7}$$

C is the fraction of mass of oxygen in a flow, and h_v is the reaction heat per unit mass of oxygen. The correction factor for incident radiative fluxes is assumed to be 1.0.

The position of the surface is given by the ablation rate, which is here defined as the sum of the depolymerization products. When it is assumed that all of the monomer leaves the body, the ablation rate is given by

$$\dot{m} \equiv \rho_0 \frac{ds}{dt} = A_p \int_s^{s+\theta} \rho_l(\xi, t) \exp\left(-\frac{E}{RT_l}\right) d\xi \quad (8)$$

where ρ_0 is some reference density; the position of the surface is given by

$$s = \int_0^t \frac{ds}{dt} dt \quad (9)$$

At the interface between the gel layer and the solid layer, both temperatures are equal, that is,

$$T_l = T_m = T_2 \quad (10)$$

On the other hand, heat flux balance across the interface can be expressed as

$$-k_2 \frac{\partial T_2}{\partial x} = -k_l \frac{\partial T_l}{\partial x} - \rho_m h_m \frac{d}{dt}(s+\theta) \quad (11)$$

where ρ_m is the mean density at the interface and is defined as $\rho_m = (\rho_1 + \rho_2)/2$. Furthermore, in Eq. (11), it is assumed that the incident radiative flux is not absorbed at the interface.

For taking the heat sink into account at the backface, the boundary condition is expressed as

$$-k_2 \frac{\partial T_2}{\partial x} + \pi \sum_{v=m}^{m'} (I - r_b) I_{T,2,v} = \rho_{hs} C_{p,hs} \delta_{hs} \frac{\partial T_2}{\partial t} \quad (12)$$

where ρ_{hs} , $C_{p,hs}$, and δ_{hs} represent the density, the specific heat, and the thickness of the heat sink, respectively.

The boundary conditions for Eqs. (3) and (4) are (see Fig. 2) at the exposed surface:

$$I_{T,1} = (I - r_{s,e}) I_e + r_{s,i} I_{R,1} \quad (13)$$

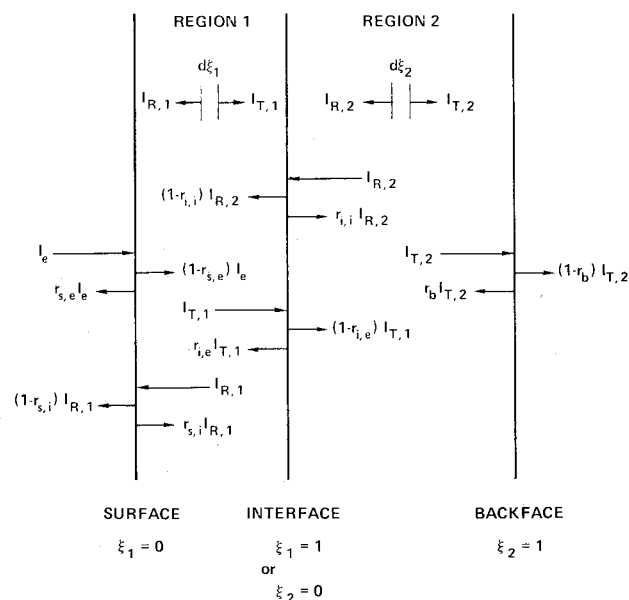


Fig. 2 Illustration of radiative transfer model.

at the interface:

$$I_{R,1} = r_{i,e} I_{T,1} + (I - r_{i,i}) I_{R,2} \quad (14)$$

$$I_{T,2} = (I - r_{i,e}) I_{T,1} + r_{i,i} I_{R,2} \quad (15)$$

at the backface:

$$I_{R,2} = r_b I_{T,2} \quad (16)$$

Initial Conditions

A prescribed initial temperature profile T_i is smaller than T_m , so that the gel layer does not exist initially. For this reason, until the surface temperature T_w reaches to T_m , the governing equations for a single-layer model are first solved, and it is assumed that the ablation does not occur. Once T_w is higher than T_m , the gel layer begins to develop and the ones for a two-layer model are solved. Therefore, we define the initial conditions as

$$T(x, 0) = T_i \quad (17)$$

$$s = \theta = 0 \quad (18)$$

The initial growing rate of the gel layer is given by the surface energy balance at $T_w = T_m$. That is,

$$-\left(k_2 \frac{\partial T_2}{\partial x}\right)_s = q_0 + q_{rad} - \rho_2 h_m \frac{d\theta}{dt} \quad (19)$$

The thickness θ of the gel layer is given by integrating of the equation of $\dot{\theta}$ from $t = t_m$ to $t = t$. That is,

$$\theta = \int_{t_m}^t \frac{d\theta}{dt} dt \quad (20)$$

Numerical Calculation

For heat conduction problems involving surface recession, it is convenient to use a coordinate system that is fixed at the moving surface. The spatial coordinate x is transformed into ξ_i ($i = 1$ or 2) by the following expressions. Within the gel layer:

$$\xi_1 = \frac{x - s(t)}{\theta(t)} \quad (21)$$

and within the solid layer:

$$\xi_2 = \frac{x - [s(t) + \theta(t)]}{L(t)} \quad (22)$$

$\xi_1 = 0$ indicates the exposed surface, $\xi_1 = 1$ or $\xi_2 = 0$ the interface, and $\xi_2 = 1$ the backface. After transformation to constant boundaries, the system of equations is solved by both an implicit finite-difference method for a system of partial differential equations and the Runge-Kutta-Gill method for a system of ordinary differential equations.

In the transformed equations, the ablation rate \dot{m} (or recession rate \dot{s}), $\dot{\theta}$, and $I_{T,1}$ (or $I_{R,1}$) at the exposed surface are three of the unknown variables. By assuming $\dot{\theta}$ and $I_{T,1}$ (or $I_{R,1}$) and taking \dot{m} as a parameter, the next relation can be obtained by solving the governing equations:

$$T_w = F(\dot{m}) \quad (23)$$

On the other hand, T_w and \dot{m} are correlated by introducing another chemical relation:

$$T_w = G(\dot{m}) \quad (24)$$

Table 1 Properties of Teflon

Property	Value	Dimension	Reference
k_1	$(21.04 - 3.34 \times 10^{-2} T/K + 1.39 \times 10^{-5} T^2/K^2) \times 10^{-4}$	$\text{cal} \cdot \text{cm}^{-1} \cdot \text{s}^{-1} \cdot \text{K}^{-1}$	6
k_2	$(1.2 \times 1.467 \times 10^{-2} T/K) \times 10^{-4}$	$\text{cal} \cdot \text{cm}^{-1} \cdot \text{s}^{-1} \cdot \text{K}^{-1}$	6
$C_{p,1}$	$0.216 + 0.156 \times 10^{-3} T/K$	$\text{cal} \cdot \text{g}^{-1} \cdot \text{K}^{-1}$	6
$C_{p,2}$	$0.123 + 0.3733 \times 10^{-3} T/K$	$\text{cal} \cdot \text{g}^{-1} \cdot \text{K}^{-1}$	6
ρ_1	$2.07 - 7 \times 10^{-4} T/K$	$\text{g} \cdot \text{cm}^{-3}$	6
ρ_2	$2.119 + 7.92 \times 10^{-4} T/K - 2.105 \times 10^{-6} T^2/K^2$	$\text{g} \cdot \text{cm}^{-3}$	6
K_1	0.22	cm^{-1}	9
K_2	0.056	cm^{-1}	9
S_1	$\leq 10^{-6}$	cm^{-1}	9
S_2	18	cm^{-1}	9
$r_{s,e}$	0.053 (if $T_w > T_m$), 0.071 (if $T_w \leq T_m$)		9
$r_{s,i}$	0.39 (if $T_w > T_m$), 0.50 (if $T_w \leq T_m$)		9
$r_{i,e}$	0.023		9
$r_{i,i}$	0.17		9
r_b	0.80		9
n_1	1.25		9, 13
n_2	1.36		9, 13
ϵ	0.1		10
H_p	$424 - 6.67 \times 10^{-2} T/K$	$\text{cal} \cdot \text{g}^{-1}$	11
h_m	14	$\text{cal} \cdot \text{g}^{-1}$	12
h_v	5.66×10^3	$\text{cal} \cdot \text{g}^{-1}$	8
E	7.56×10^4	$\text{cal} \cdot \text{mole}^{-1}$	6
A_p	3.1×10^{19}	s^{-1}	6

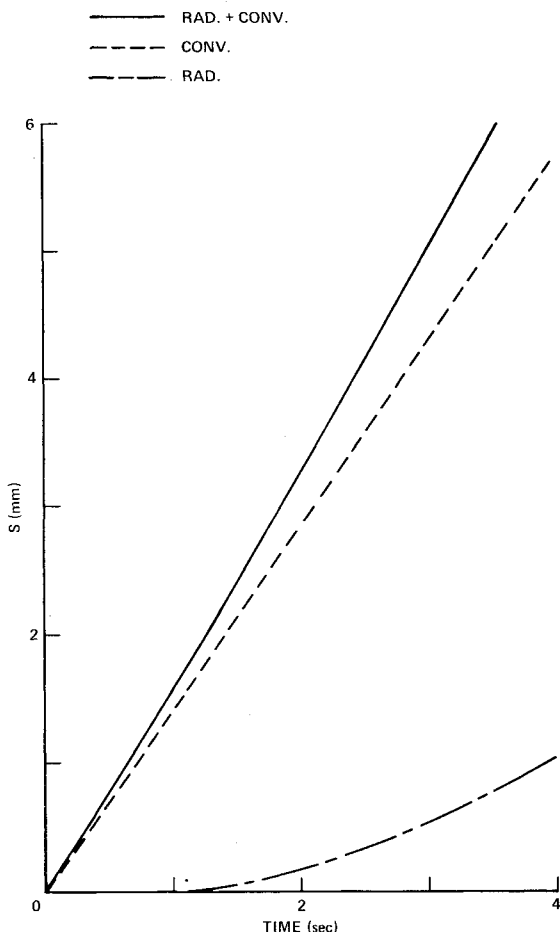


Fig. 3 History of recession depth: $H_0 = 1000 \text{ cal/g}$, $q_0 = 100 \text{ cal/s/cm}^2$, $q_r = 250 \text{ cal/s/cm}^2$.

Thus, two relations are obtained that give the desired solutions for \dot{m} and T_w . The desired \dot{m} and T_w can be found graphically or numerically from Eqs. (23) and (24). Then the governing equations are again solved by using the obtained \dot{m} and T_w , and at last all solutions are obtained. The thermal and optical properties of Teflon used in this calculation are shown in Table 1.

Results and Discussion

One of the main purposes of this investigation is to investigate the effect of radiative heating on the thermal field in the heat shield. In the sample calculations from Figs. 3-7, $L_0 = 1.0 \text{ cm}$, $H_0 = 1000 \text{ cal/g}$, $q_0 = 100 \text{ cal/s/cm}^2$, and $q_r = 250 \text{ cal/s/cm}^2$. (Of the incident radiation, we estimate that 96.5% penetrates and 3.5% is absorbed at the surface.) It is assumed that the backface is insulated.

Figure 3 shows the recession depth history. There is a great difference between the radiative heating only and other cases. This result is caused by the fact that a greater part of an incident radiative heating comes through the surface and penetrates into the material. The heat which is absorbed at the surface is very small. Therefore, the surface temperature increases very slowly compared with other cases and is lower than in other cases; consequently, the recession velocity is much smaller than in other cases.

Figures 4 and 5 show the history of the thickness of the gel layer and the growing rate, respectively. In the case of the radiative heating only, the gel layer is much thicker than in other cases. This may be explained as follows. The internal temperature increases mainly due to the absorption of the incident radiation, while the surface recession velocity in the case of the radiative heating only is much smaller than in other cases. Therefore, the thickness keeps on increasing. In the case of the combined radiative and convective heating, the surface recession is large, so the gel is very thin. However, because of the incident radiation, the thickness does not become constant. On the other hand, in the case of the

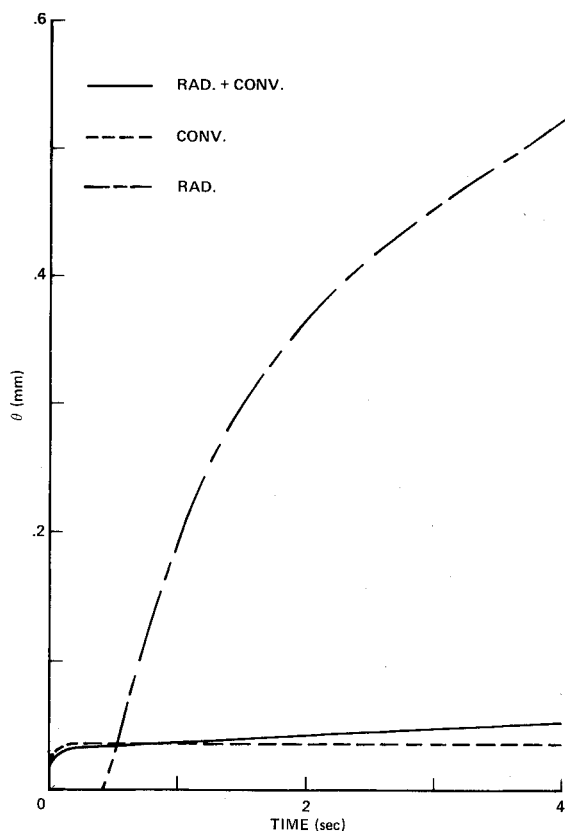


Fig. 4 History of the thickness of gel layer: $H_0 = 1000$ cal/g, $q_0 = 100$ cal/s/cm², $q_r = 250$ cal/s/cm².

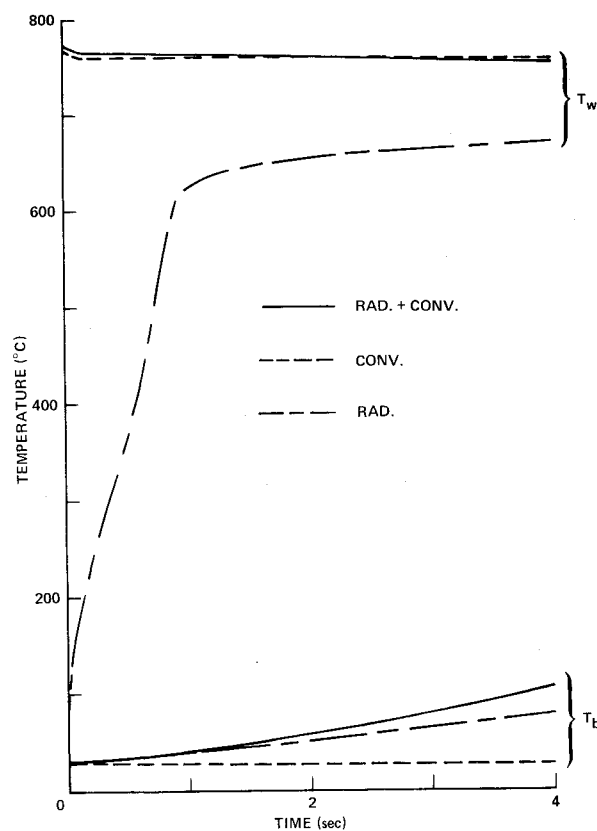


Fig. 6 Surface and backface temperature history: $H_0 = 1000$ cal/g, $q_0 = 100$ cal/s/cm², $q_r = 250$ cal/s/cm².

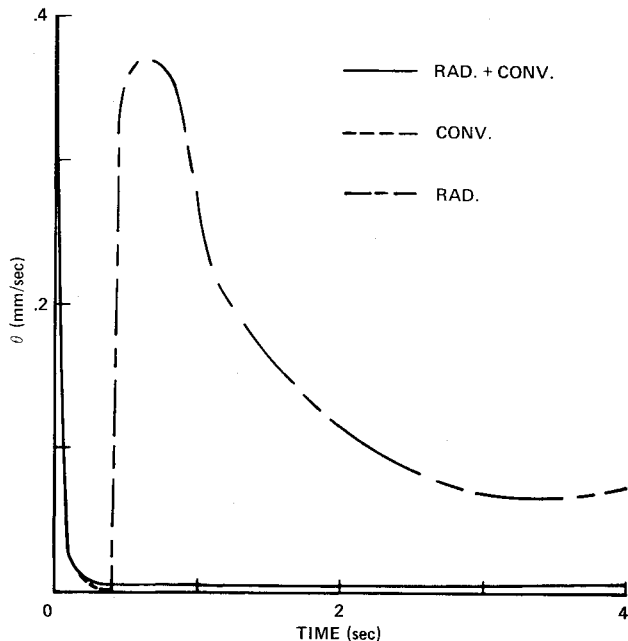


Fig. 5 Growing rate of the gel layer: $H_0 = 1000$ cal/g, $q_0 = 100$ cal/s/cm², $q_r = 250$ cal/s/cm².

convective heating only, it becomes almost constant at an early time.

Figure 6 shows the history of the surface and the backface temperatures. In the cases of the combined heating and the convective heating only, the surface temperature increases abruptly and becomes almost constant very soon. On the other hand, in the case of the radiative heating only, it increases much more slowly than in other cases. The backface temperature does not increase in the case of the convective

heating only; whereas it continues to increase in other cases. This seems to be caused by the fact that only a small part of the incident radiation is absorbed at the surface and that a greater part of it penetrates into the material. The radiation scattered deep into the material becomes trapped, thereby increasing the internal temperature. The backface temperature in the case of the radiative heating only is lower than in the case of the combined heating. This seems to be caused by the difference of the surface recession velocity. The thickness of the material in the former case is much greater than in the latter case. Therefore, the radiation is trapped on the way and only a part of it reaches the backface. In the case of convective heating only, the backface temperature does not rise because of the low thermal diffusivity of Teflon.

Figures 7a-7c show the instantaneous temperature distribution. As previously mentioned, the greater part of the rise of the internal temperature (except near the surface) seems to be caused by the scattering and the absorption of the incident radiation. When the thermal thickness is defined as

$$\delta = \frac{l}{T_w} \int_s^{L_0} T dx \quad (25)$$

in the case of the convective heating only, it is much smaller than in other cases. The surface temperature is influenced mainly by the convective heating, whereas the internal temperature distribution is influenced mainly by the radiative heating.

The comparison with another theory⁷ is shown in Fig. 8. The difference seems to be caused not only by the differences in physical properties, but also by the difference in the evaluation of the incident radiation. In Ref. 7, the effect of the incident radiation is taken into account in the gel layer, but not in the solid phase. Therefore, the temperature at the backface in Ref. 7 does not rise as does that in the present analysis.

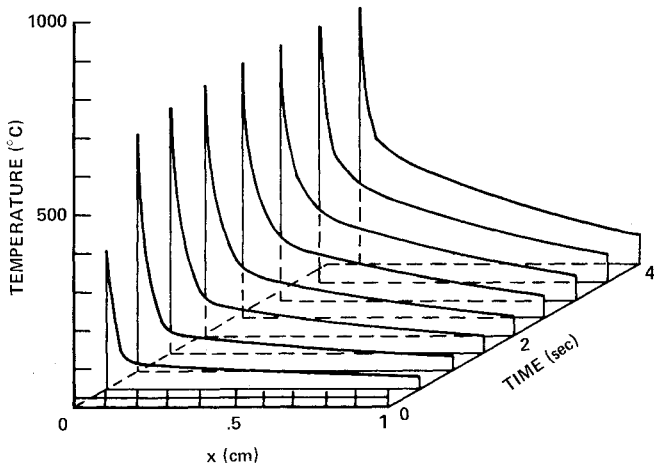


Fig. 7a Temperature distribution as a function of time and position with radiative heating only: $H_0 = 1000 \text{ cal/g}$, $q_r = 250 \text{ cal/s/cm}^2$.

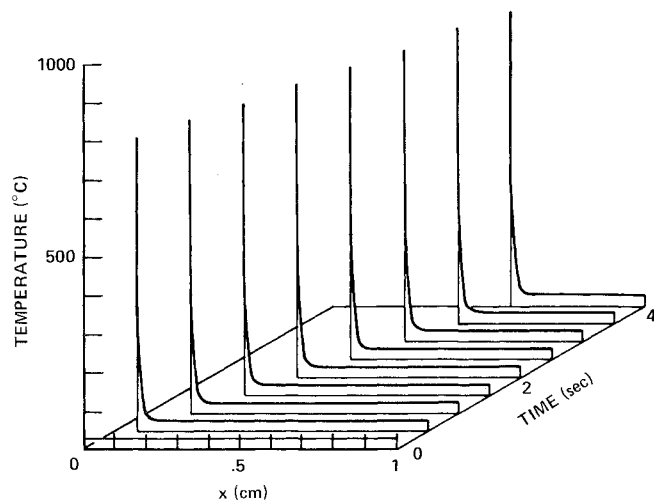


Fig. 7b Temperature distribution as a function of time and position with convective heating only: $H_0 = 1000 \text{ cal/g}$, $q_0 = 100 \text{ cal/s/cm}^2$.

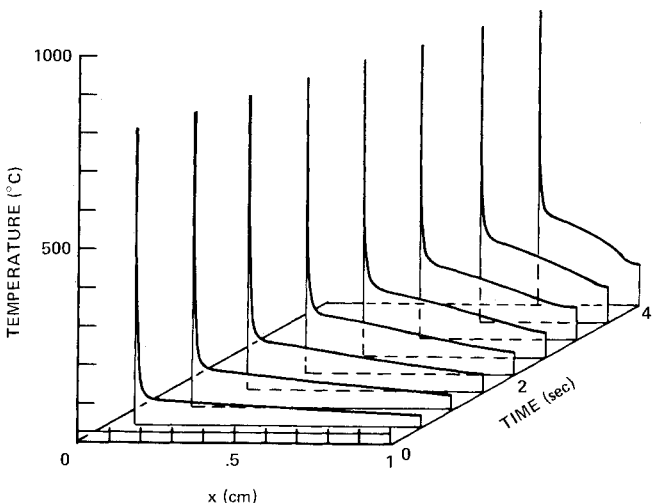


Fig. 7c Temperature distribution as a function of time and position with combined radiative and convective heating: $H_0 = 1000 \text{ cal/g}$, $q_0 = 100 \text{ cal/s/cm}^2$, $q_r = 250 \text{ cal/s/cm}^2$.

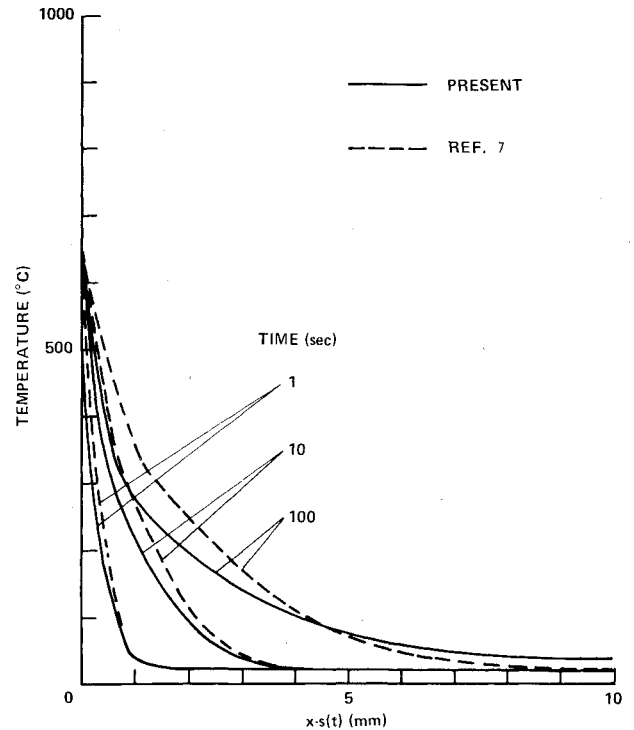


Fig. 8 Temperature distribution in an ablating body: $H_0 = 2127 \text{ cal/g}$, $q_0 = 15.24 \text{ cal/s/cm}^2$, $q_r = 1.69 \text{ cal/s/cm}^2$.

Conclusion

Investigation of the high-temperature behavior of Teflon was taken as a basis for an analytical model of the transient ablation of Teflon under the condition in which the intense radiation is coupled with the convective heating. The growing process of the gel layer and the instantaneous internal temperature distribution seem to be influenced significantly by the incident radiation; whereas the surface temperature does not seem to be influenced by it. Only near the surface, the convective heating influences the internal temperature distribution. In the case of the convective heating only, the steady-state ablation seems to be reached at a very early time, while it does not seem to be reached when the incident radiation is accounted for. The results of the present calculations confirm that the optical transmittance of both the amorphous zone (gel layer) and the crystalline zone cannot be neglected in considering the transient ablation under the condition of the radiative heating.

Acknowledgment

The author would like to express his gratitude to P. R. Nachtsheim and J. T. Howe of NASA Ames Research Center for their initiation of this work and for their very useful comments. He also wishes to thank the anonymous reviewers for their valuable discussions.

References

- ¹Nachtsheim, P. R., Peterson, D. L., and Howe, J. T., "Reflecting and Ablating Heat Shields for Radiative Environments," AAS Paper 71-147; also *Advances in the Astronautical Sciences*, Vol. 29, II, 1971, pp. 253-264.
- ²Howe, J. T., Green, M. J., and Weston, K. G., "Thermal Shielding by Subliming Volume Reflectors in Convective and Intense Radiative Environments," *AIAA Journal*, Vol. 11, July 1973, pp. 989-994.
- ³Howe, J. T. and McCulley, L. D., "Volume-Reflecting Heat Shield for Entry Into the Giant Planet Atmospheres," AIAA Paper 74-669, 1974.
- ⁴Clark, B. L., "A Parametric Study of the Transient Ablation of Teflon," *Journal of Heat Transfer*, Vol. 94 C, 1972, pp. 347-354.

⁵Arai, N., "A Study of Transient Thermal Response of Ablation Materials," Institute of Space and Aeronautical Science, University of Tokyo, ISAS Rept. 544, Sept. 1976.

⁶Holzknrecht, B., "An Analytical Model of The Transient Ablation of Polytetrafluoroethylene Layers," *International Journal of Heat and Mass Transfer*, Vol. 20, June 1977, pp. 661-668.

⁷Kindler, K., "Experimentelle Untersuchung des Ablationsverhaltens von einfachen Körpern unterschiedlicher Nasenform und Materialzusammensetzung," Deutsche Forschungs- und Versuchsanstalt für Luft- und Raumfahrt, Institut für Angewandte Gasdynamik, Köln, DLR-FB 76-08, Jan. 1976.

⁸Pope, R. B., "Simplified Computer Model for Predicting the Ablation of Teflon," *Journal of Spacecraft and Rockets*, Vol. 12, Feb. 1975, pp. 83-88.

⁹Congdon, W. M., "Reflecting Heat-Shield Entry Analysis Computer Program for Planetary Probes," AIAA Paper 73-714, 1973.

¹⁰Nicolet, W. E., Howe, J. T., and Mezines, S. A., "Outer Planet Probe Entry Thermal Protection: Part II: Heat-Shielding Requirements," AIAA Paper 74-701, 1974.

¹¹Kemp, N. H., "Surface Recession Rate of an Ablating Polymer," *AIAA Journal*, Vol. 6, Sept. 1968, pp. 1790-1791.

¹²Wentink, T., Jr., "High Temperature Behavior of Teflon," Avco Research Lab., Rept. 55, 1959.

¹³MaCane, D. I., "Tetrafluoroethylene Polymers, Polytetrafluoroethylene," *Encyclopedia of Polymer Science and Technology*, Vol. 13, John Wiley & Sons Inc., New York, 1970, pp. 623-654.

From the AIAA Progress in Astronautics and Aeronautics Series..

EXPERIMENTAL DIAGNOSTICS IN COMBUSTION OF SOLIDS—v. 63

Edited by Thomas L. Boggs, Naval Weapons Center, and Ben T. Zinn, Georgia Institute of Technology

The present volume was prepared as a sequel to Volume 53, *Experimental Diagnostics in Gas Phase Combustion Systems*, published in 1977. Its objective is similar to that of the gas phase combustion volume, namely, to assemble in one place a set of advanced expository treatments of the newest diagnostic methods that have emerged in recent years in experimental combustion research in heterogenous systems and to analyze both the potentials and the shortcomings in ways that would suggest directions for future development. The emphasis in the first volume was on homogenous gas phase systems, usually the subject of idealized laboratory researches; the emphasis in the present volume is on heterogenous two- or more-phase systems typical of those encountered in practical combustors.

As remarked in the 1977 volume, the particular diagnostic methods selected for presentation were largely undeveloped a decade ago. However, these more powerful methods now make possible a deeper and much more detailed understanding of the complex processes in combustion than we had thought feasible at that time.

Like the previous one, this volume was planned as a means to disseminate the techniques hitherto known only to specialists to the much broader community of research scientists and development engineers in the combustion field. We believe that the articles and the selected references to the current literature contained in the articles will prove useful and stimulating.

339 pp., 6 x 9 illus., including one four-color plate, \$20.00 Mem., \$35.00 List

TO ORDER WRITE: Publications Dept., AIAA, 1290 Avenue of the Americas, New York, N.Y. 10019